JOURNAL OF THEORETICAL
AND APPLIED MECHANICS
1, 36, 1998

TEXTURES INDUCED BY THE ROLLER BURNISHING PROCESS

WIKTOR GAMBIN

Institute of Fundamental Technological Research, Polish Academy of Sciences

e-mail: wgambin@ippt.gov.pl

The roller burnishing of machine elements improves considerably their smoothness and resistance to corrosion and wear. This process delays an initiation and propagation of microcracks in the surface layer of the burnished elements. It is due to induced high compressive residual stresses and increased yield stresses of the layer. The plastic anisotropy that appears in the layer is caused by texture development during the plastic yield of the material However, the opposite effect is frequently observed in the engineering practice (Pahlitzsch and Krohn, 1966): too many cycles of the burnishing process may cause a softening and finally a peeling and cracking of the surface layer. A description of the above "seizing effect" has been given recently by Gambin (1996a,b). To find the reason for softening of the burnished surface, the textures induced in metal surface layers after successive cycles of the process are analysed in the paper. On the basis of the classical solution to rolling of rigid-perfectly plastic half-space (Collins, 1972), velocity gradients in the plastic zone are determined. Next, a previously proposed model of crystal plastic behaviour (Gambin, 1991a,b) enables one to calculate crystallographic lattice reorientations, and to predict a texture development in the burnished surface layer. The texture obtained after the first pass of the roller is different from those observed after rolling of thin metal sheets. Successive passes of the roller gradually destroy the first pass texture. It confirms practical observations; i.e., the burnishing of machine elements through a few passes under a higher load gives better results than the burnishing through many powerless passes.

Key words: textures, burnishing, plastic yield

1. Introduction

The roller burnishing of machine elements increases their resistance to the destructive effects of physical and chemical factors appearing during exploitation processes. A high load applied to the roller causes the plastic yield in a metal surface layer. In result the anisotropic hardening and compressive

residual stresses appear in the layer. They prevent initiation and propagation of microcracks in the material. An estimation of residual stresses in the burnished layer one can find in the paper by Gambin (1996c). In the present paper, the reasons for the induced plastic anisotropy are discussed. Microscopic observations indicate two of them: elongation of metallic grains leading to the *morphological texture* and reorientation of crystalline lattices leading to the *crystallographic texture*. For pure metals the last one has a decisive influence on appearance and development of plastic anisotropy. Let us explain this phenomenon. Because the plastic yield of a single crystal appears as a result of glides on a finite number of slip systems, a grain behaviour is plastically anisotropic. During the plastic yield, the slip planes and slip directions rotate together with the crystallographic lattice. In crystal aggregates, one can observe appearance of privileged lattice orientations called the crystallographic texture. When the plastic yield proceeds along the same deformation path, the texture becomes stronger and stronger. Concluding, a texture analysis of burnished surface layers enables one to predict the final plastic properties of the layer, and it allows for control of the burnishing process. The basic information about the texture analysis one can find in the book by Bunge (1982). Practical applications of the texture analysis were described in the book edited by Wenk (1985). A brief review of typical deformation textures was given in the paper by Dillamore and Roberts (1965), as well as, in the paper by Hu (1974).

On the other hand, it appears that the texture analysis enables one to explain the *seizing effect* that may take place during the burnishing process (Pahlitzsch and Krohn, 1966): after too many cycles of burnishing, softening and finally peeling and cracking of the burnished surface occur. A description of the *seizing effect* was given recently by Gambin (1996a,b). In the present paper, the influence of many cycles of the burnishing process on the final texture is analysed. On the macroscopic level, the roller burnishing process is considered as a frictionless rolling of rigid cylinder on the rigid-perfectly plastic half-space. Basing on the classical solution (Collins, 1972), a velocity field in the plastic zone is assumed. The corresponding velocity gradients of plastically deformed surface layer are calculated in the next section. When assuming the Taylor model of polycrystal behaviour to find lattice reorientations of crystalline aggregate, it is enough to know the macroscopic velocity gradient acting on this aggregate (Taylor, 1938). The Taylor model and the description of crystal plastic behaviour proposed by Gambin (1991a,b) enable one to predict the burnishing textures. These textures are compared with the rolling textures of thin metal sheets. The obtained results suggest avoiding of multiple burnishing of the same machine element.

2. Deformation of burnished surface layer

Consider a rolling of rigid cylinder on a rigid-perfectly plastic half-space with a constant speed V. According to the Collins model based on the slip-line theory, the rolled surface undergoes a cumulative horizontal displacement in the direction of the roller motion. The simplified slip line field, in the case of frictionless loading by the vertical force W and the horizontal force H. is shown in the Fig.1a.

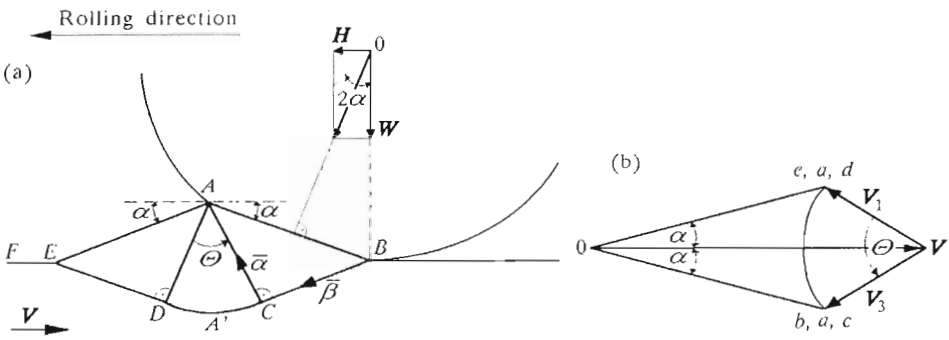

Fig. 1. Classical solution for frictionless rolling: (a) – slip-line field, (b) – hodograph

In the considered case the deformation is fully determined by one parameter – the angle α that describes the slope of plastic wave to the rolled surface. Assume that the roller is rotating about a fixed point. and the rolled half-space is moving under the roller at a constant speed V. Let us observe deformation of a small material element passing through the plastic zone. From the corresponding hodograph (Fig.1b), it yields that the velocity fields in the triangles ADE and ABC are constant and they smoothly change in the circular fan ACD. It means that a material element under the line FE crossing the line DE undergoes the simple shear in the direction V_1. Passing through the triangle ADE this element remains undeformed up to the line AD, where it undergoes the simple shear in the direction of resultant velocity $V_2(\theta) - V_1$. Crossing the line AC, the material element undergoes the simple shear in the vertical direction parallel to the vector $V_3 - V_1$. In the triangle ABC this element remains undeformed up to the line BC, where it undergoes the simple shear in the direction $-V_3$ (opposite to V_3). Notice, that the element undergoes a complex deformation only in the circular fan ACD. However, the resultant velocity in this area $V_2(\theta) - V_1$ differs only slightly from the resultant vertical velocity $V_3 - V_1$ in the triangle ABC. For that reason one

can assume, that the considered material element undergoes to the following deformation processes:

1. Simple shear in the direction V_1 along the line DE
2. Simple shear in the vertical direction $V_3 - V_1$ in the triangle ACD
3. Simple shear in the direction $-V_3$ along the line BC.

To describe these three simple shears, let us introduce the material $\{X_i\}$ and the spatial $\{x_i\}$ system of Cartesian coordinates. The axes X_i and x_i are opposite to the rolling direction, X_2 and x_2 are normal to the rolled surface, while X_3 and x_3 are parallel to the transverse direction. Because, on the macroscopic level, we have to do with the plane strain, the coordinates X_3 and x_3 are neglected in this section. For each of the simple shears a current position $\{x_1, x_2\}$ of the material particle $\{X_1, X_2\}$ is given by the rule

$$\begin{aligned} x_1(X_1, X_2; t) &= A_{11}(t)X_1 + A_{12}(t)X_2 \\ x_2(X_1, X_2; t) &= A_{21}(t)X_1 + A_{22}(t)X_2 \end{aligned} \tag{2.1}$$

where

$$A_{ij}(t) = a_{ij}t + (1-t)\delta_{ij} \tag{2.2}$$

for $0 \leq t \leq 1$.

To find the coefficients a_{ij} for each of the simple shears, it is enough to determine the final position $p_0 = \{x_1^0, x_2^0\}$ and $p_s = \{x_1^s, x_2^s\}$ of the two material particles: $P_0 = \{X_1^0, X_2^0\}$ which does not change the position, and $P_s = \{X_1^s, X_2^s\}$ which undergoes the considered simple shear.

Ad 1. *The simple shear along the line* DE

Introducing $\{X_1^0, X_2^0\} = \{x_1^0, x_2^0\} = \left\{1, \tan\left(\frac{\pi}{4} - \alpha\right)\right\}$, $\{X_1^s, X_2^s\} = \{1, 0\}$ and $\{x_1^s, x_2^s\} = \{(1 - \tan\alpha)/(1 + \tan^2\alpha), \tan\alpha\ (1 - \tan\alpha)/(1 + \tan^2\alpha)\}$ to Eqs (2.1) and (2.2), one can obtain

$$\begin{aligned} a_{11} &= \frac{1 - \tan\alpha}{1 + \tan^2\alpha} \cong 1 - \alpha - \alpha^2 \\ a_{12} &= -\frac{(1 + \tan^2\alpha)^2}{1 + \tan^2\alpha}\frac{\tan\alpha}{1 - \tan\alpha} \cong -\alpha - \alpha^2 \\ a_{21} &= \frac{1 - \tan\alpha}{1 + \tan^2\alpha}\tan\alpha \cong \alpha - \alpha^2 \\ a_{22} &= -\frac{1 + \tan\alpha + 2\tan^2\alpha}{1 + \tan^2\alpha} \cong 1 + \alpha + \alpha^2 \end{aligned} \tag{2.3}$$

Ad 2. *The simple shear in the vertical direction* AA'

Now introduce $\{X_1^0, X_2^0\} = \{x_1^0, x_2^0\} = \{0, \tan\alpha\}$, $\{X_1^s, X_2^s\} = \{1, 2\tan\alpha\}$ and $\{x_1^s, x_2^s\} = \{1, 0\}$, to Eqs (2.1) and (2.2). In this case

$$\begin{aligned} a_{11} &= 1 & a_{12} &= 0 \\ a_{21} &= -2\tan\alpha \cong -2\alpha & a_{22} &= 1 \end{aligned} \tag{2.4}$$

Ad 3. *The simple shear along the line* BC

Let $\{X_1^0, X_2^0\} = \{x_1^0, x_2^0\} = \left\{1, \tan\left(\frac{\pi}{4} - \alpha\right)\right\}$ to Eqs (2.1), (2.2), $\{X_1^s, X_2^s\} = \{1, 0\}$ and
$\{x_1^s, x_2^s\} = \{(1 - \tan\alpha)/(1 + \tan^2\alpha), \tan\alpha\,(1 - \tan\alpha)/(1 + \tan^2\alpha)\}$.
From Eqs (2.1) and (2.2) it follows

$$\begin{aligned} a_{11} &= \frac{1 + \tan\alpha + 2\tan^2\alpha}{1 + \tan^2\alpha} \cong 1 + \alpha + \alpha^2 \\ a_{12} &= -\frac{\tan\alpha}{1 - \tan\alpha} \cong -\alpha - \alpha^2 \\ a_{21} &= \frac{1 - \tan\alpha}{1 + \tan^2\alpha}\tan\alpha \cong \alpha - \alpha^2 \\ a_{22} &= \frac{1 - \tan\alpha}{1 + \tan^2\alpha} \cong 1 - \alpha - \alpha^2 \end{aligned} \tag{2.5}$$

Consider the velocity field and the strain rate field for the above three cases. The velocity of the material particle $\{X_1^s, X_2^s\}$, during the motion prescribed by Eqs (2.1) and (2.2), is given by the relation

$$V_i(X_j) = \frac{\partial x_i}{\partial t} = (a_{ij} - \delta_{ij})X_j \tag{2.6}$$

Then, when material particles pass through the point $\{x_1^s, x_2^s\}$ on the line DE, AA' or BC the velocity field in a vicinity of this point has the form

$$v_i(x_j) = (a_{ij} - \delta_{ij})x_j \tag{2.7}$$

The corresponding strain rate tensor and spin tensor are as follows

$$d_{ij} = \frac{1}{2}(v_{ij} + v_{ji}) = \begin{bmatrix} a_{11} - 1 & \frac{1}{2}(a_{12} + a_{21}) \\ \frac{1}{2}(a_{12} + a_{21}) & a_{22} - 1 \end{bmatrix} \tag{2.8}$$

and

$$\omega_{ij} = \frac{1}{2}(v_{ij} - v_{ji}) = \begin{bmatrix} 0 & \frac{1}{2}(a_{12} - a_{21}) \\ \frac{1}{2}(a_{21} - a_{12}) & 0 \end{bmatrix} \tag{2.9}$$

It is enough to introduce Eqs (2.3) ÷ (2.5) into Eqs (2.8) ÷ (2.9), to obtain:
— in the triangle ADE

$$\begin{aligned} d_{11} &= -\frac{1+\tan\alpha}{1+\tan^2\alpha}\tan\alpha \cong -\alpha - 2\alpha^2 \\ d_{12} &= d_{21} = \frac{-2\tan^2\alpha}{(1+\tan^2\alpha)(1+\tan\alpha)^2} \cong -2\alpha^2 \\ d_{22} &= \frac{1+\tan\alpha}{1+\tan^2\alpha} \cong \alpha + 2\alpha^2 \\ \omega_{12} &\cong -\alpha \end{aligned} \tag{2.10}$$

— in the circular fan ACD

$$\begin{aligned} d_{11} &= 0 \qquad & d_{12} &= d_{21} \cong -\alpha \\ d_{22} &= 0 \qquad & \omega_{12} &\cong \alpha \end{aligned} \tag{2.11}$$

— in the triangle ABC'

$$\begin{aligned} d_{11} &= \frac{1+\tan\alpha}{1+\tan^2\alpha}\tan\alpha \cong \alpha + 2\alpha^2 \\ d_{12} &= d_{21} = \frac{-2\tan^2\alpha}{(1+\tan^2\alpha)(1+\tan\alpha)^2} \cong -2\alpha^2 \\ d_{22} &= \frac{1+\tan\alpha}{1+\tan^2\alpha} \cong -\alpha - 2\alpha^2 \\ \omega_{12} &\cong -\alpha \end{aligned} \tag{2.12}$$

Since the angle α takes small values during the process, one can keep in Eqs (2.10) ÷ (2.12) only linear terms with respect to α.

According to our assumptions the final deformation of the burnished layer appears due to three simple shears along the lines: DE, AA' and BC. The present considerations aim at finding the final texture of pollycrystalline material caused by the above three simple shears. Mariatty et al. (1992) compared the textures caused by the simple shear in the x_2 direction (the line AA' in Fig.1a) with the textures caused by pure shear in the same direction.

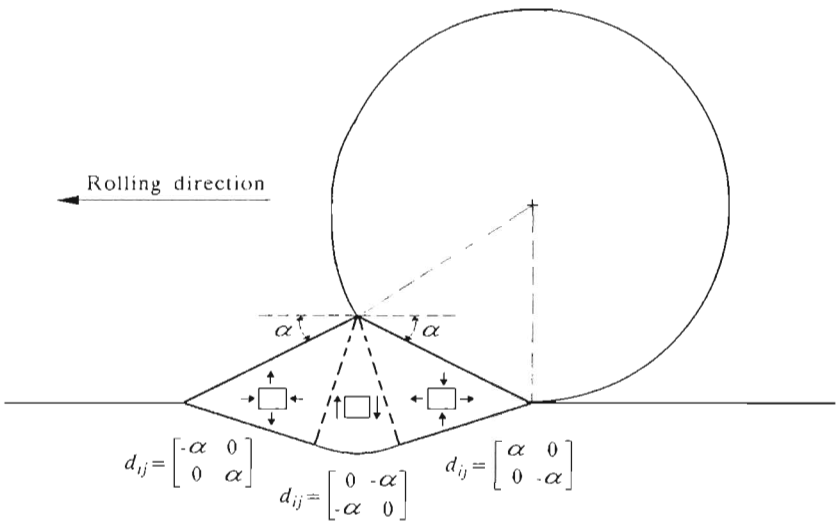

Fig. 2. Three deformation steps in the roller burnishing process

The corresponding (111) pole figures were similar, although the simple shear texture was not intensively developed as the pure shear textures. Moreover, the simple shear textures were slightly turned due to rotation of the principal axes of strain rate tensor. The influence of this rotation on the final texture is very little. The commonly assumed model of rolling textures proposed by Calnan and Clews in 1950 (see: Dillamore and Roberts, 1965 or Honeycombe. 1984) takes into account the above fact and it assumes that the rolling textures are due to tension in the rolling direction and compression in the vertical direction, or due to pure shear in the direction rotated through the angle of 45° about the x_3 axis (the lines BC and DE in Fig.1a). Concluding, one can assume that the spin ω_{ij} exerts a very little influence of the final burnishing texture, and consider the three pure shears on the lines DE, AA' and BC'. instead of the simple shears. It is equivalent to the assumption that the burnished surface layer undergoes the following three deformations (see Fig.2):

— the "inverse rolling" in the triangle ADE, with

$$d_{ij} = \begin{bmatrix} -\alpha & 0 \\ 0 & \alpha \end{bmatrix} \tag{2.13}$$

— the pure shear in the circular fan ACD, with

$$d_{ij} = \begin{bmatrix} 0 & -\alpha \\ -\alpha & 0 \end{bmatrix} \tag{2.14}$$

— the rolling in the triangle ABC, with

$$d_{ij} = \begin{bmatrix} \alpha & 0 \\ 0 & -\alpha \end{bmatrix} \tag{2.15}$$

The above three steps of the roller burnishing process have a decisive influence on the plastic anisotropy development in metal surface layers.

3. Burnishing textures

A sequence of the three deformation processes represented by Eqs (2.13) ÷ (2.15) considerably changes a microstructure of the burnished layer. The crystallographic lattices of grains, rotating during a plastic yield, induce a strong plastic anisotropy. To determine lattice reorientations of a single grain, it is necessary to know the velocity gradient acting on this grain (Asaro, 1983). According to the Taylor model of polycrystal behaviour (Taylor, 1938), one can assume that grain velocity gradients are the same and equal to the macroscopic one. This macroscopic velocity gradient is a sum of the strain rate tensor d_{ij} and the total spin ω_{ij}. However, the grains of the burnished layer undergo local plastic spins ω_{ij}^{p} referred to the lattice frame. Then, to find the lattice reorientation ω_{ij}^{L}, it is enough to take the difference between the total spin ω_{ij} and a local plastic spin ω_{ij}^{p}. Consider a single grain with a local stress tensor σ_{ij} acting on this grain. Denote by s_{ij} a deviator of the tensor σ_{ij}. The yield condition, five constitutive relations between the deviatoric strain rate tensor d_{ij} and s_{ij}, and three constitutive relations between the plastic spin ω_{ij}^{p} and s_{ij}, enable one to formulate a complete system of the equations determining the lattice reorientations during a deformation process (see Appendix).

To model the deformation texture development, the numerical code prepared by Gambin and Barlat (1993) is used. The code is based on the rate independent crystal plasticity formulation proposed by Gambin (1991), (1992). The examples of calculated textures after various metallurgical processes for f.c.c. (face cubic crystalline) and b.c.c. (body center crystalline) materials (Gambin, 1996c) show a good agreement with the experimental results. To

predict the burnishing textures a deformed material element of the metal surface layer is assumed to be composed of 106 grains. The grain aggregate is initially an isotropic one. It means that the initial lattice orientations are uniformly distributed in the orientation space. The results are shown with the help of (111) and (100) pole figures. As previously, the axis x_1 is assumed in the rolling direction, x_2 - in the direction normal to the rolled surface and x_3 - in the transverse direction. The bove reference frame and the initial isotropic distribution of 106 grains are shown in the Fig.3.

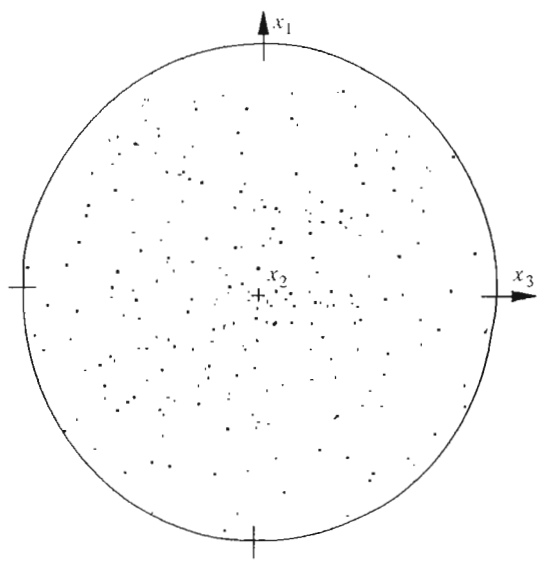

Fig. 3. Initial distribution of 106 grains and the assumed reference frame

The final deformation of material is determined by the angle $\alpha = 15°$. This angle is small enough to assume the linear approximation (2.13) $\div$ (2.15) of Eqs (2.10) $\div$ (2.12). A virtual strain rate increment is assumed. For the same of simplicity, only the case of f.c.c. metals is considered. The (111) and (100) pole figures after the first pass of the roller are shown in Fig.4. They indicate strong plastic anisotropy induced in the surface layer. However, they are different from the rolling textures observed in thin sheets (Fig.5). After the second and third passes of the roller the initial burnishing texture became increasingly fuzzy (Fig.6). It is on the contary to the case of rolling of thin sheets, in which reinforcement of textures is observed. Particulary large texture weakening appears when the second pass is in the direction opposite to the assumed in the first pass.

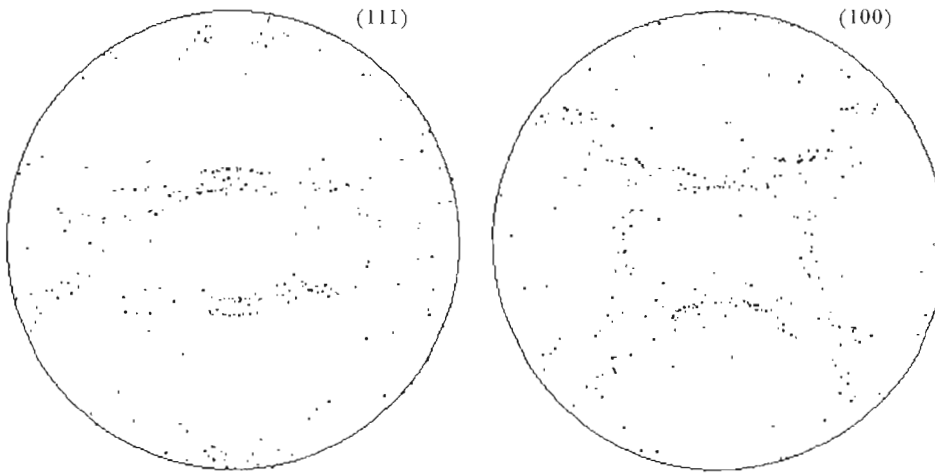

Fig. 4. The (111) and (100) pole figures after the first pass of the roller in the burnishing process with $\alpha = 15°$

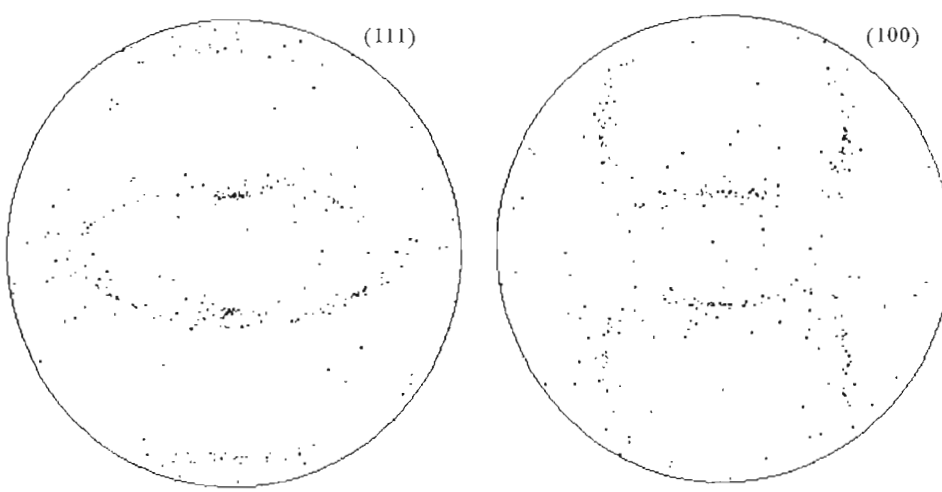

Fig. 5. The (111) and (100) pole figures after rolling of thin sheet with 40% thickness reduction

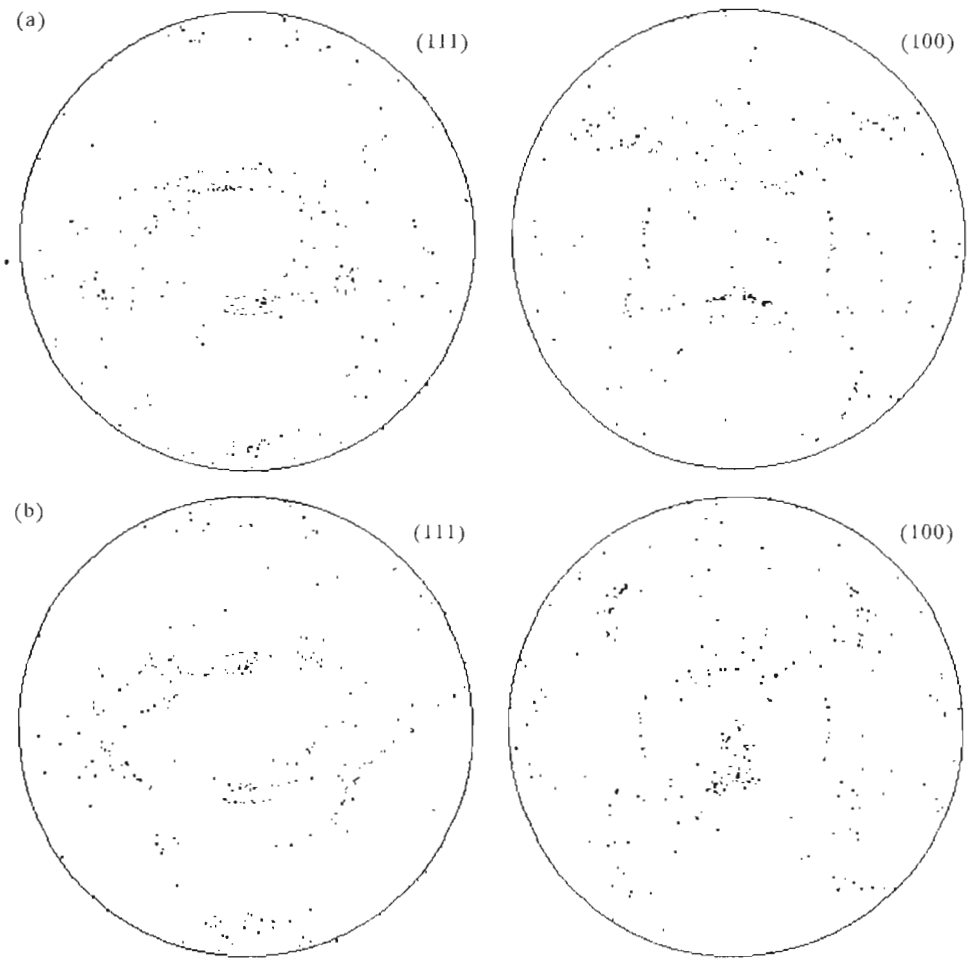

Fig. 6. The (111) and (100) pole figures in the burnishing process with $\alpha = 15°$. (a) – after the second pass of the roller, (b) – after the third pass of the roller

4. Conclusions

During the roller burnishing process the compressive residual stresses and an anisotropic hardening appear in metal surface layers. Both factors prevent an early initiation and propagation of microcracks in the material. The induced plastic anisotropy is due to a texture development during the deformation process. This process may be decomposed into the three stages:

1. *"Inverse rolling" process* – when the material fibres in the rolling di-

rection are compressed, and the normal ones to the rolled surface are extended at the same strain rate

2. *Pure shear process* – when the material fibres normal to the burnished surface are sheared in the rolling direction

3. *Rolling process* – when the material fibres in the rolling direction are extended, and the normal ones to the rolled surface are compressed with the same strain rate.

The texture of the burnished surface layer after the first pass of the roller is distinct, but different from that obtained after rolling of a thin sheet. The opposite character of the stages 1 and 3, and as a little influence of the stage 2 on the texture cause the plastic anisotropy induced during the first pass of the roller to be destroyed after the next passes. The following conclusion, important for the engineering practice can be, therefore, drawn: the burnishing of machine element in a few passes under a higher load gives the better result than the burnishing in many powerless passes. Too many cycles of the burnishing process may lead to peeling and cracking of surface layers. The above conclusion was confirmed by the experimental tests done by Pahlitzsch and Krohn (1966) and was taken into account in the engineering practice (Przybylski, 1987).

Appendix: Determination of crystallographic lattice reorientations for plastically deformed polycrystals

Consider a plastically deformed polycrystalline element composed of several hundred grains. A crystallographic lattice of each grain may be described in a frame of three orthogonal vectors. Three Euler angles $\{\varphi_1^0, \varphi_2^0, \varphi_3^0\}$ will give an initial orientation of the frame with respect to a fixed system of coordinates $\{x_1, x_2, x_3\}$. During the polycrystal deformation the lattice frames rotate at a spin $\omega_{ij}^L = \dot{R}_{ik} R_{jk}$, where the rotation matrix R_{ij} depends on the initial lattice orientation described by the angles $\{\varphi_1^0, \varphi_2^0, \varphi_3^0\}$, and the current Euler angles $\{\varphi_1, \varphi_2, \varphi_3\}$, while $\dot{R}_{ik}$ is the time derivative of R_{ij}. To know the texture development in the considered polycrystalline element, it is enough to know $\dot{\varphi}_1$, $\dot{\varphi}_2$ and $\dot{\varphi}_3$ at each moment of the deformation process. Below a complete system of equations for the vector $\{\dot{\varphi}_1, \dot{\varphi}_2, \dot{\varphi}_3\}$ is given (see: Gambin, 1991a).

Let $\{\widehat{m}_i^{(r)}, \widehat{n}_j^{(r)}\}$, for $r = 1, 2, ..., M$, be a system of slip systems of a single grain in the lattice frame. Here, $\widehat{m}_i^{(r)}$ is the versor of slip direction, and $\widehat{n}_j^{(r)}$ – the versor normal to the corresponding slip plane. Of course, $\widehat{m}_i^{(r)}$ and $\widehat{n}_j^{(r)}$ are fixed lattice parameters. The critical shear stress on the rth slip system is equal to $k_c^{(r)}$ and does not change during a plastic yield of the crystal. When the deformation process occurs, the slip systems rotate together with the lattice frame according the rules: $m_i^{(r)}(\varphi_k) = R_{ij}(\varphi_k)\widehat{m}_j^{(r)}$ and $n_i^{(r)}(\varphi_k) = R_{ij}(\varphi_k)\widehat{n}_j^{(r)}$. Denote by $P_{ij}^{(r)}(\varphi_k)$ and $W_{ij}^{(r)}(\varphi_k)$, the symmetric and antisymmetric parts of the diade $A_{ij}^{(r)}(\varphi_k) = m_i^{(r)}(\varphi_k)n_j^{(r)}(\varphi_k)$, respectively. Let σ_{ij} will be the Cauchy stress acting on the crystal. Then, the following system of equations describes the behaviour of rigid-perfectly plastic crystals:

- Plasticity condition (the regularized Schmid law with an integer exponent $1 \leq n \leq 20$; the physical meaning of the parameter n was given by Gambin and Barlat (1997)

$$\sum_{r=1}^{M} \Big[\frac{s_{kl}A_{kl}^{(r)}}{k_c^{(r)}}\Big]^{2n} = m \tag{A.1}$$

  where the non-dimensional, constant for a given crystalline lattice, parameter m depends on the critical shear stresses $k_c^{(r)}$ and the lattice parameters $\widehat{m}_i^{(r)}$ and $\widehat{n}_j^{(r)}$, as follows

$$m \equiv \frac{1}{M}\sum_{s=1}^{M}\sum_{r=1}^{M}\Big[2\frac{k_c^{(s)}}{k_c^{(r)}}\widehat{P}_{kl}^{(s)}\widehat{P}_{kl}^{(r)}\Big]^{2n} \tag{A.2}$$

  and $\widehat{P}_{ij}^{(r)}$ is the symmetric part of the diade $\widehat{m}_i^{(r)}\widehat{n}_j^{(r)}$

- Five constitutive equations for components of the strain rate deviator (with a yield function λ)

$$d_{ij} = \lambda\sum_{r=1}^{M}\frac{1}{k_c^{(r)}}\Big[\frac{s_{kl}A_{kl}^{(r)}}{k_c^{(r)}}\Big]^{2n-1}P_{ij}^{(r)} \tag{A.3}$$

- Three constitutive equations for the total spin components (composed of the local plastic spin – the first term of the right-hand side, and the lattice spin – the second term)

$$\omega_{ij} = \lambda\sum_{r=1}^{M}\frac{1}{k_c^{(r)}}\Big[\frac{s_{kl}A_{kl}^{(r)}}{k_c^{(r)}}\Big]^{2n-1}W_{ij}^{(r)} + \dot{R}_{jk}R_{jk} \tag{A.4}$$

Let us assume that the global velocity gradient (d_{ij} plus ω_{ij}) is known. Then, from nine equations (A.1) $\div$ (A.4), one can find: five components of the stress deviator s_{ij}, the yield function λ, and three time derivatives of the Euler angles: $\dot{\varphi}_1$, $\dot{\varphi}_2$ and $\dot{\varphi}_3$. To obtain the pole figures for a given deformation process, it is necessary to divide the whole deformation time into small time-steps. Next, it is necessary to repeat successively the above calculations at each step for all grains of the polycrystalline element. Integration of the vector $\{\dot{\varphi}_1, \dot{\varphi}_2, \dot{\varphi}_3\}$ over all time-steps gives the final lattice orientation for each grain of the polycrystalline element.

Acknowledgement

The paper was supported by the State Committee for Scientific Research (KBN) under grant No. PB 3 P402 016 07.

References

1. ASARO J.R., 1983, Crystal Plasticity, *J. Appl. Mech.*, **50**, 921-934
2. BUNGE H.J., 1982, *Texture Analysis in Material Sciences - Mathematical Methods*, Butterworths, London
3. DILLAMORE I.L., ROBERTS W.T., 1965, Preferred Orientations in Wrought and Annealed Metals, *Metall. Rev.*, **10**, 271-380
4. COLLINS I. F., 1972, A Simplified Analysis of the Rolling of a Cylinder on a Rigid/Perfectly Plastic Half-Space, *Int. J. Mech. Sci.*, **14**, 1-14
5. GAMBIN W., 1991a, Plasticity of Crystals with Interacting Slip Systems, *Eng. Trans.*, **39**, 3-4, 303-324
6. GAMBIN W., 1991b, Crystal Plasticity Based on Yield Surfaces with Rounded-Off Corners, *ZAMM* **71**, T 265-T 268
7. GAMBIN W., 1992, Refined Analysis of Elastic-Plastic Crystals, *Int. J. Solids Structures*, **29**, 16, 2013-2021
8. GAMBIN W., 1996a, Seizing Effect in the Roller Burnishing Process, *Acta Physica Polonica A*, **86**, 3, 371-375
9. GAMBIN W., 1996b, Plastic Analysis of Metal Surface Layers Undergoing the Roller Burnishing Process, *Eng. Trans.*, **44**, 471-481
10. GAMBIN W., 1996c, Finite Element Analysis of Textured Materials, *J Theor Appl. Mech.*, **34**, 4, 713-732
11 GAMBIN W., BARLAT F , 1997, Modelling of Deformation Texture Development, *Proc. 4th Int. Symp. on Plasticity and Its Current Applications - PLASTICITY'93*, Baltimore/USA July 1993 - will appear in *International Journal of Plasticity*

12. HONEYCOMBE R.W.K., 1984, *The Plastic Deformations of Metals*, Arnold Ltd., London

13. HU H., 1974, Texture of Metals, *Textures*, 233-258

14. MARIATTY A.M., DAWSON P.R., LEE Y.S., 1992, A Time Integration Algorithm for Elasto-Viscoplastic Cubic Crystals Applied to Modelling Polycrystalline Deformations, *Int. J. Num. Meth. Engng*, **35**, 1565-1588

15. MATHUR K.K., DAWSON P.R., 1989, On Modelling the Development of Crystallographic Texture in Bulk Forming Processes, *Int. J. Plast.*, **5**, 67-94

16. PAHLITZSCH G., KROHN P., 1966, Über das Glattwalzen zylindrischer Werkstüke im Einstechverfahren, *Werkstattstechnik*, Nr.1

17. PRZYBYLSKI W., 1987, *Burnishing Technology* (in Polish), WNT, Warszawa

18. TAYLOR G.I., 1938, Plastic Strain in Metals, *J. Inst. Metals*, **62**, 1, 307-324

19. WENK H.R. (edit.), 1985, *Preferred Orientations in Deformed Metals and Rocks: An Introduction to Modern Texture Analysis*, Academic Press Inc., Orlando, Florida

Tekstury wywołane procesem nagniatania

Streszczenie

Proces nagniatania tocznego części maszyn znacznie zwiększa ich gladkość oraz odporność na korozję i zużycie. Ponadto powoduje zmniejszenie inicjacji i propagacji mikroszczelin w warstwie wierzchniej nagniatanych elementów. Następuje to w wyniku wprowadzenia znacznych resztkowych naprężeń ściskających i anizotropowego podwyższenia granicy plastyczności warstwy. Anizotropia plastyczna, która pojawia się w warstwie, spowodowana jest ewolucją tekstury podczas plastycznego plynięcia nagniatanego materialu. W pracy analizowane są tekstury warstw wierzchnich metali wywołane procesem nagniatania. Na podstawie znanego rozwiązania problemu walcowania sztywno-idealnie plastycznej pólprzestrzeni (Collins, 1972) określono pole prędkości odkształceń w strefie uplastycznionej. Następnie zastosowano uprzednio zaproponowany model plastycznego zachowania się kryształów (Gambin, 1991) do obliczenia reorientacji sieci krystalograficznej i określenia rozwoju tekstury w nagniatanej warstwie. Okazalo się że tekstura, która pojawia się po pierwszym cyklu nagniatania jest inna niż obserwowana po procesie walcowania cienkich blach. Kolejne cykle nagniatania stopniowo niszczą teksturę pierwszego cyklu. Prowadzi to do następującego wniosku: zbyt wiele cykli nagniatania może prowadzić do oslabienia, a w rezultacie do spękania i złuszczenia warstwy wierzchniej nagniatanego materialu. Ze zjawiskiem tym spotykamy się w praktyce inżynierskiej (Przybylski, 1987).

Manuscript received November 12, 1996; accepted for print September 18, 1997